MICROINDENTATION BEHAVIOR UNDER QUASI-STATIC AND CREEP MODES OF CARBON NANOTUBES (CNTs)-REINFORCED THERMOSETTING POLYMERS

F. Chapalain[1], M. Drissi-Habti[1]*, JF Feller[2], I. Pillin[2], Y. Guéguen[3], JC Sangleboeuf[3], T. Bourouina[4]

[1] *PRES LUNAM, IFSTTAR, Monitoring, Auscultation and Scientific Calculation DEPT. (MACS), CS4 Route de Bouaye, 44344 Bouguenais Cedex, France*
[2] *LARMAUR, ERL 6274 Bât 10B - Université de Rennes 1 Campus de Beaulieu 35042 Rennes Cedex, France*
[3] *LIMATB EA-4250. Université de Bretagne-Sud. Centre de Recherche rue de Saint Maudé - BP92116 56321 Lorient Cedex, France*
[4] *ESIEE, Laboratoire ESYCOM, EA 2552, Cité Descartes BP 99 93162 Noisy-Le-Grand, France*

*For correspondences: * monssef.drissi-habti@ifsttar.fr*

Keywords: Carbon nanotubes (CNTs), creep, nanocomposite, instrumented micro-indentation, mechanical characterization, viscoelasticity

Abstract

Due to their exceptional mechanical properties and their low density, carbon nanotubes are ideal fillers for the mechanical reinforcement of polymeric matrices. When properly dispersed, literature reports that a small amount of carbon nanotubes is able to enhance the mechanical behaviour of thermosetting matrices. In this work, vinylester and epoxy resins reinforced by small weight fractions of carbon nanotubes were processed. The microstructure was checked by scanning electron microscopy. Micro-indentation tests under quasi-static loading and creep were carried out to compare non-reinforced and CNTs-reinforced resins. Quasi-static micro-indentation tests show a noticeable but not-spectacular increase of the local Young's modulus and hardness of CNTs-reinforced resins. On the reverse, creep under micro-indentation show a significant first stage creep on CNTs-reinforced resins which is increasing with the increase of CNTs weight's ratio.

1 Introduction

Composite materials based on polymeric matrices are interesting alternatives for many structural uses, due to their higher stiffness-to-weight ratio in comparison with metallic materials as well as their improved corrosion-resistance. However, in some demanding industrial applications such as off-shore wind turbines, high speed transportation, there is a need for higher performance than what is exhibited up to date.

Carbon nanotubes (CNTs) are good candidates for polymer reinforcement as they exhibit excellent mechanical properties (Table 1). If correctly dispersed in the matrix, a small fraction in weight is able to enhance the stiffness of the polymer.

Density	1,8g/cm^3
Diameter	1- 20 nm
Specific area	10 – 20m²/g
Young's modulus	0,3 – 1TPa
Tensile strength	10 – 60GPa
Electrical conductivity	10^{6}S/m
Thermal conductivity	2000W.m^{-1}K^{-1}
Thermal expansion coefficient	Negligible

Table 1. Carbon nanotubes properties

Many teams have already worked on reinforcement of epoxy matrices by adding CNTs and contradictory results were reported. For instance, with 0.5wt% of CNTs, Ma et al. [1] increased the Young's modulus of their reinforced resins by 9%. Sumfleth et al. [2], with 0.5wt% of CNTs in an epoxy resin too, observed an improvement of 14% of the Young's modulus and Song et al. [3] observed a 20% increase. In 2003, Bai and Allaoui [4] showed an increase of the Young's modulus of 62% for an epoxy resin reinforced with 0.5wt% of CNTs.

On the reverse, a significant enhancement of mechanical properties is not always observed experimentally. Indeed some teams observed only a 5% increase of the stiffness of the reinforced epoxy like Gojny et al. [5], while Hernandez-Perez [6] observed a 10% decrease of the Young's modulus of a nano-reinforced epoxy resin. By adding 2wt% of CNTs in the epoxy matrix, Guo at al. [7] observed a decrease of 6% of the Young's modulus.

This contrast in the final properties can mainly be explained by both the quality as well as the dispersion of CNTs within the matrices. Indeed, commercially available CNTs can present defects and impurities that reduce their mechanical properties. Moreover, Van der Waals interactions that are acting between CNTs tend to agglomerate them as nano-bundles irregularly dispersed within the matrix. In the case these nano-aggregates become micro-aggregates, they may turn to mechanical defects that significantly decrease the mechanical properties of the matrix. The issue of dispersion of CNTs within resins is widely discussed in the literature. It has been shown that large fractions of CNTs are harder to disperse correctly in the matrix. Thus, for both, providing ease of processing as well as for obvious technological targets, only small weight fractions of CNTs were used in the present work.

In this study, instrumented micro-indentation technique under quasi-static mode is used to evaluate the impact of adding 0.2wt% of CNTs on the mechanical properties of epoxy and vinylester resins. The local Young's modulus and the Hardness of both non-reinforced and CNTs-reinforced resins were measured and compared. These results are discussed with regards to observations under optical and scanning electron microscopy (SEM).

We then present the results of 15 minutes as well as 50 hours micro-indentation creep tests on both monolithic and CNTs-reinforced vinylester and epoxy. Through these results, we intend to highlight the reinforcing effects of CNTs in the matrix.

2 Material and testing methods
2.1 Materials
Two systems of nanocomposites were manufactured. The first one is based on a vinylester resin commercially named Derakane 470-S36, cured with a methyl-ethyl ketone peroxide hardener (MEKP Curox M-102) and a cobalt accelerator. The carbon nanotubes (Graphistrength®, Arkema) are provided as dispersion in an epoxy matrix and put in a pellet shape. The second composite studied is based on epoxy matrix.

2.2 Nanocomposite processing

The Graphistrength® is firstly heated in vinylester resin and then mixed by standard propeller mixer to obtain a first solution were pellets are still present. As recommended by both Graphistrength® handling guide and bibliography (Gojny et al. [8]), a three rolls mill (Figure 1) was used to disperse CNTs within the matrix. This method is enabling good splitting of the pellet and a good dispersion of CNTs. After 10 minutes of mixing, the material was heated to reduce viscosity and degassed for 15 minutes. The hardener was then mixed by hand to the solution and placed into a mould covered by a thin layer of anti-adhesive sticker. To ensure the plate remains plane, an upper mould with weight was used during curing 1h at 80°C.
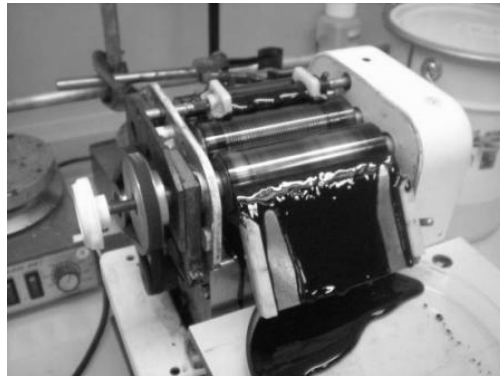

Figure 1. Nanocomposite processing with a three rolls mill

2.3 Characterization

Scanning Electron Microscopy (SEM JEOL 58000LV) was used to investigate the microstructure of the nanocomposites and to evaluate the state of dispersion of CNTs. The mechanical properties (Young's modulus, Hardness and viscoelasticity) were measured by instrumented micro-indentation (Shimadzu DUH-211S). In this test a load is applied in the investigated material by a very hard tip with a precisely known shape. In our case, a pyramidal tip shape named Berkovich tip and a spherical tip shape were used. The local Young's modulus and the Hardness are obtained by analyzing the response curve of the material to the loading/unloading cycle as illustrated in Figure 2. By repeating the measurements at several locations on the whole surface of the samples, the averaged values that are obtained can compare to the macroscopic value of the Young's modulus, for example. The local Young's modulus is deduced from the maximal depth and slope of the unloading curve through the formulas (1) and (2) (Oliver and Pharr, [9]).

In the case of creep tests, the maximal force programmed is kept for a moment, then creep is observed and a viscoelastic coefficient can be calculated through expression (3). In our case, the maximal force was held for 15 minutes with Berkovich tip and 50h with the spherical tip.
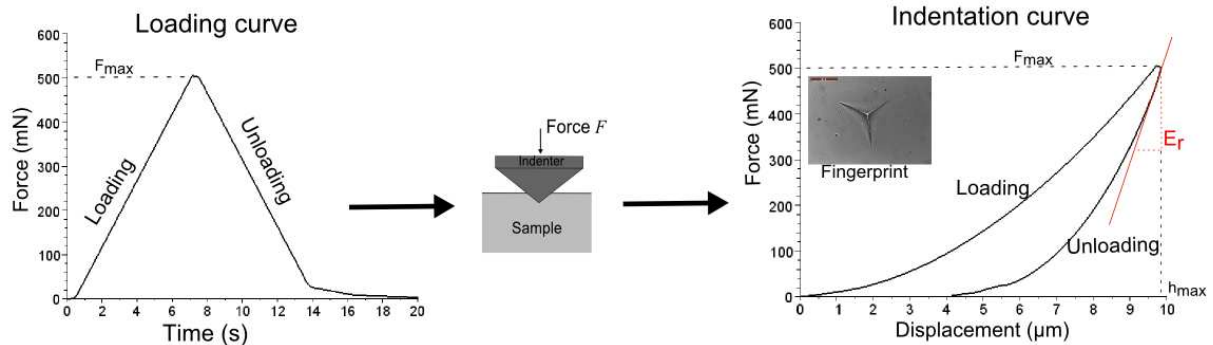

Figure 2. Illustration of the instrumented micro-indentation test

$$\frac{1}{E_r} = \frac{1-v^2}{E} + \frac{1-v_i^2}{E_i} \tag{1}$$

$$H = \frac{F_{max}}{A_p} \tag{2}$$

$$C = \frac{h_2 - h_1}{h_1} \times 100 \tag{3}$$

Were E_r is the reduced modulus deducted from the slope of the unloading curve and from A_p
E, υ are local Young's modulus and Poisson's coefficient of the tested material
E_i, υ_i are Young's modulus and Poisson's coefficient of the indenter
h is the hardness of the tested material
A_p the projected area of the indentation footprint
C is the viscoelasticity coefficient
h_1 is the depth of indentation when the maximal load is reached
h_2 is the depth of indentation at the end of the holding, just before unloading

The shear creep compliances were measured by indentation creep test. In the case of a linear elastic homogenous material, the relation of Sneddon (1965) [10] is establishing the link between the applied load, P_e, and the indentation depth, h, at the time, t.

$$h^n(t) = \frac{1-v}{\mu} \times F \times P_e(t) \tag{4}$$

Where μ is the shear modulus, v the Poisson's ratio, F and n are constant values related to the tip geometry.

In the case of viscoelastic materials, the elastic parameters μ and v have to be replaced by their viscoelastic time-dependant counterpart υ and G, which is possible in the case of a monotonic increase of the area of contact. Lee and Radok (1960) [11] achieved this substitution using the method of functional equations.

$$h^n(t) = \frac{1-\upsilon}{F} \times \int_0^t J(t-s) \frac{\partial P(s)}{\partial s} \, ds \tag{5}$$

Where J is a Laplace-Carson transform of the creep shear compliance and υ a constant as the shear flow is incompressible and predominant at large time. We will take υ=0.5. The creep indentation loading is given by the step loading relation

$$P(t) = P_0 H(t) \tag{6}$$

Where H is the Heaviside function, so expression (6) becomes

$$h^n(t) = \frac{1-\upsilon}{F} P_0 \times \int_0^t J(t-s) \, ds \tag{7}$$

And
$$J(t) = \frac{F}{1-\upsilon} P_0 h^n(t)$$
(8)

In the case of a cylindrical flat-punch, of radius a, the parameters of this equation are: $F = 4a$ and $n = 1$. The shear compliance J can be decomposed into an elastic component $J_e = 1/\mu$ and a time-dependent component J_v, this latter corresponding to the viscoelastic contribution (viscous flow and delayed elasticity):

$$J(t) = J_e + J_v(t)$$
(9)

During an indentation-creep test, the elastic component, J_e, can be measured during the loading phase, if the indentation machine is calibrated; and J_v during the creep, without any calibration, as the load is constant.

This equipment operating in the micro-indentation range has been developed by [12] and [13]. The load, applied using a piezoelectric actuator, is ranging between 0.01 and 50 N. The penetration depth is measured with two laser sensors having a resolution of 20 nm. The load fluctuation is less than ±12 mN. The samples were indented at room temperature (20+/-1°C), using a cylindrical flat-punch made of tungsten carbide ($a = 187.5$ µm). The load was applied within 15+/-0.1 s, up to 23 N, and kept constant during 180 000 s (50 hours). As the indentation machine is not calibrated, the measurements are only focused on J_v.

3 Structural investigations

Pull-outs of CNTs were observed through the SEM as shown in Figure 3a. This mechanism is a proof of existence of a reinforcing effect induced by the addition of CNTs to the matrix. Some aggregates of carbon nanotubes were also observed as shown in Figure 3b. Indeed, as reported in the literature, it is pretty tough to get large effective dispersion of carbon nanotubes.
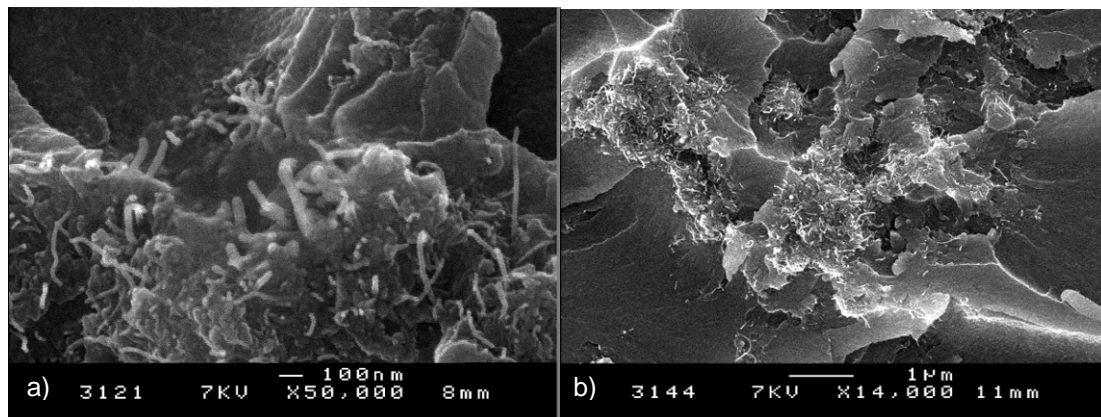

Figure 3. Carbon nanotubes dispersed in a vinyl ester matrix a) pull-outs, b) agglomerate

4 Quasi-static micro-indentation tests

Loading/unloading to a programmed maximal force cycle is applied on tested samples without holding the maximal force. Both monolithic and nano-reinforced resins are tested. The response curves of quasi-static micro-indentation tests are shown on Figure 4, for monolithic and reinforced vinylester and epoxy resins. It can be seen that for the force range and the loading speed tested, though the stiffening displayed by CNTs-reinforced resins in Figures 4a and 4b, no definitive conclusion can be drawn regarding the values of the local Young's modulus and the Hardness, though a slight stiffening is recorded (Figures 4).
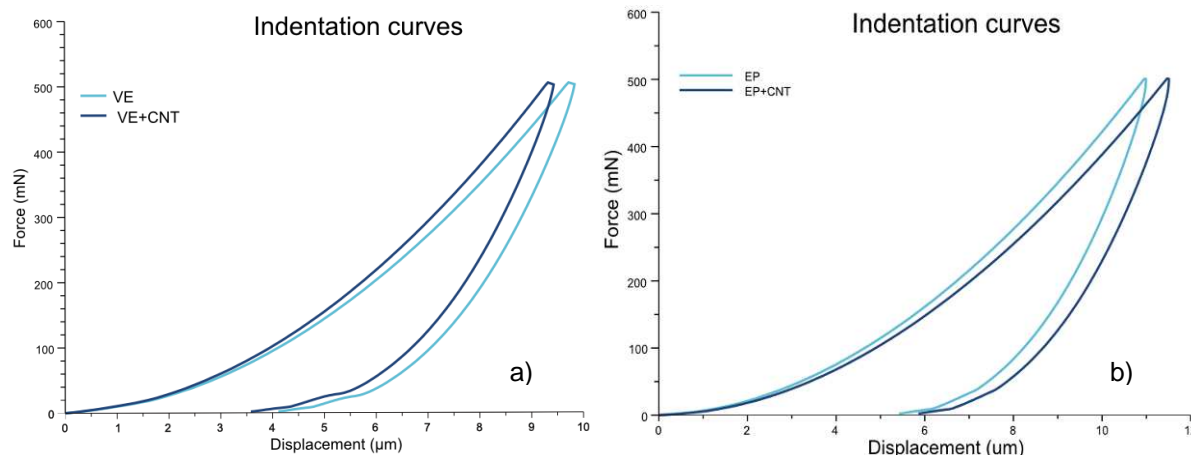
Figure 4. Indentation response curves of monolithic and nano-reinforced a) vinyl ester and b) epoxy resins

5 Creep micro-indentation test results

Figure 5 shows 15 minutes micro-indentation creep curves for monolithic and reinforced vinylester and epoxy resins. A change in the viscoelastic behavior is observed when comparing the monolithic and CNTs-reinforced matrices behaviors. This can be related to a stiffening mechanism of the matrix induced by the presence of CNTs. In the case of the epoxy resin, a significant decrease as high as 14% is even recorded for the viscoelastic coefficient for the reinforced matrix as shown in Table 3.
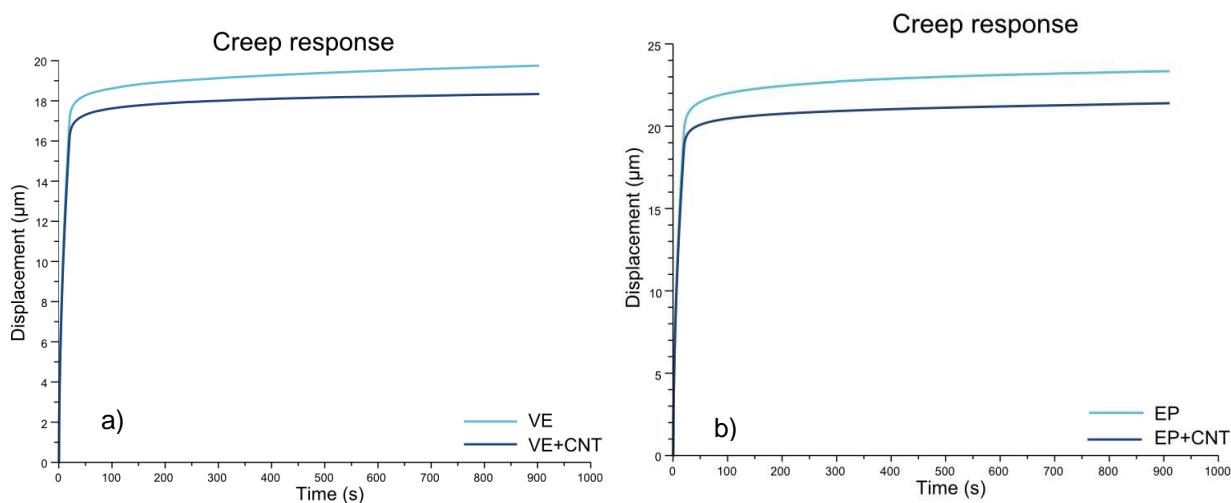

Figure 5. Indentation creep response curves of monolithic and nano-reinforced a) vinyl ester and b) epoxy resins

0,2% CNT	% Young's modulus	% Hardness	% Viscoelastic Coefficient
Vinyl ester	+10%	+6%	-4%
Epoxy	+ 4,5%	+ 20%	- 14,5%

Table 3. Evolution of the mechanical properties of the nano-reinforced matrix compared to the monolithic one measured by creep indentation

When conducting 50 hours creep tests, the primary creep stage is clearly highlighted for CNTs-reinforced resins. In addition, the higher is the weight ratio of CNTs, the larger is the primary creep stage (Figure 6).
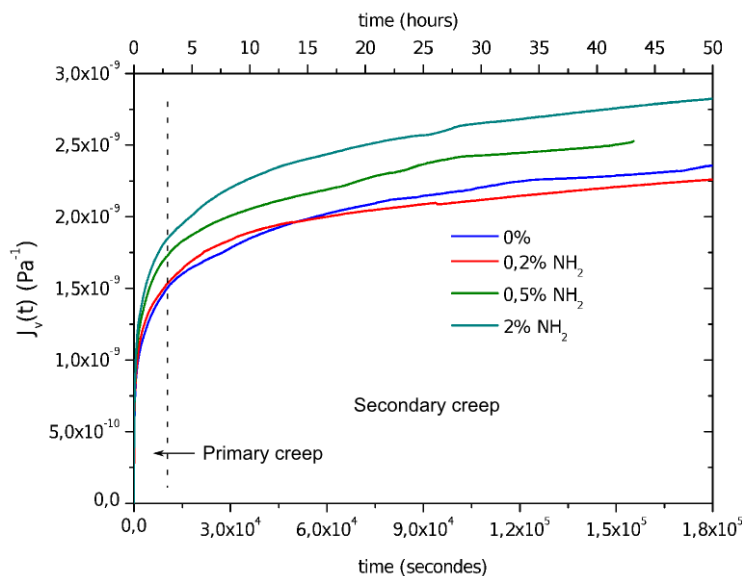
Figure 6. 50h shear creep compliance of neat and nano-reinforced epoxy obtained by indentation-creep tests

6 Conclusions

In this work, the reinforcement mechanisms following the addition of small weight ratios of CNTs to resins were evidenced. Carbon nanotubes pull-outs were observed through SEM observations.

Micro-indentation creep tests show different behaviours when comparing monolithic and CNTs-reinforced resins. An increase in the viscoelastic coefficient as high as 14% was recorded for CNTs-reinforced resins. In addition, a primary creep stage was clearly displayed by reinforced resins, for which the higher is the CNTs weight ratio, the larger is the primary creep stage. This is a clear indication of the reinforcement through the addition of CNTs.

References

[1] Ma P., Mo S., Dispersion, interfacial interaction and re-agglomeration of functionalized carbon nanotubes in epoxy composites, *Carbon,* **48**, 1824-1834, (2010).
[2] Sumfleth J., Prehn K., A comparative study of the electrical and mechanical properties of epoxy nanocomposites reinforced by CVD- and arc-grown multi-wall carbon nanotubes, *Composites Science and Technology,***70**, 173-180, (2010).
[3] Song, Y., Youn J., Influence of dispersion states of carbon nanotubes on physical properties of epoxy nanocomposites, *Carbon,* **43**, 1378 – 1385. (2005).
[4] Bai J., Allaoui A., Effect of the length and the aggregate size of MWNTs on the improvement efficiency of the mechanical and electrical properties of nanocomposites - experimental investigation , *Composites Part A: Applied Science and Manufacturing,* **34**, 689 – 694, (2003).
[5] Gojny F., Wichmann M., Influence of different carbon nanotubes on the mechanical properties of epoxy matrix composites - A comparative study, *Composites Science and Technology, 20th Anniversary Special Issue,* **65**, 2300-2313, (2005).
[6] Hernandez-Perez A., Aviles F, Effective properties of multiwalled carbon nanotube/ epoxy composites using two different tubes, *Composites Science and Technology,* **68**, 1422-1431, (2008).

[7] Guo P., Chen X., Fabrication and mechanical properties of well-dispersed multiwalled carbon nanotubes/epoxy composites, *Composites Science and Technology,* **67**, 3331–3337, (2007).

[8] Gojny F., Wichmann M, Carbon nanotube-reinforced epoxy-composites: enhanced stiffness and fracture toughness at low nanotube content, *Composites Science and Technology, Developments in carbon nanotube and nanofibre reinforced polymers,* **64**, 2363-2371, (2004).

[9] Oliver W.C, Pharr G.M., Measurement of hardness and elastic modulus by instrumented indentation: Advances in understanding and refinements to methodology, *Journal of Materials Research*, **19**, 3-20, (2004).

[10] Sneddon I.N., The relation between load and penetration in the axi-symmetric Boussinesq problem for a punch of arbitrary profile, *The International Journal of Engineering Science,* **3**, 47–57, (1965)

[11] Lee E.H., Radok J.R.M, The Contact Problem for Viscoelastic Bodies, *Journal of Applied Mechanics,* **27**, 438-444, (1960)

[12] Bernard C., Ph.D thesis, University of Rennes 1, (2006)

[13] Bernard C., Keryvin V., Indentation creep of window glass around glass transition, *Mechanics of materials*, **42**, 196-206, (2010)